論文
ANALYSIS OF UNBONDED PRESTRESSED CONCRETE STRUCTURES BY LATTICE EQUIVALENT CONTINUUM MODEL

Nattakorn BONGOCHGETSAKUL*1 Tada-aki TANABE*2
Atsushi ITOH*3 and Kongkeo PHAMAVANH*4

ABSTRACT: The application of the Lattice Equivalent Continuum Model was very successful so far in predicting the behavior of RC structures under monotonic and cyclic loading. New application of the model to the prestressed concrete components will be presented here accompanied with the formulation for embedded curved prestressing tendon. Nonlinear FEM with multilayered shell element were adopted for the analysis. LECM is also capable for shear-transfer between crack surfaces, which is exceedingly important when adopting the shell element. Finally, the model was verified by series of prestressed beams wth satisfactory results.
KEYWORDS: prestressed concrete, constitutive equation, Lattice Equivalent Continuum Model, prestressing formulation

1. INTRODUCTION

Lattice Equivalent Continuum Model [1], briefly called LECM, a constitutive equations of reinforced concrete for predicting behavior of the cracked concrete element. Basic concept of the model is to replace concrete and reinforcement of the RC element by a system of lattices, in which each corresponding lattice possesses its own uniaxial properties. Stress components relation between global stress field and those of the lattice system is considered by using a concept of Micro-plane model. The model works with stress and strain vectors on a set of planes of various orientations, so called Micro-plane. Based on the micro-plane that changes its direction according to propagation direction of the crack, stress-strain relation of corresponding lattice component can be appropriately expressed. Consequently, complicated characteristics of the cracked reinforced concrete element can be simplified. Moreover, by applying uniaxial properties to each lattice component, nonlinear behavior material even the more complicated hysteretic rules (loading-unloading behavior) of concrete and reinforcement can be independently defined. In addition, not only concrete and reinforcement that were represented by the system of lattices, an extra lattice system is also introduced to represent the contribution from shear transfer mechanism. This is one more feature of the model.

The application of the LECM is not limited to only reinforced concrete field. By introducing the prestressing tendon formulation to the LECM, a good behavior prediction of the prestressed concrete component can also be obtained and this will be shown in the later section.

In this study, a general purpose finite element analysis program which is designed for research and educational use namely FEAPpv (acronym for A Finite Element Analysis Program: Personal Version), which is written by professor R.L. Taylor of the university of California, Berkeley, was adopted for all analyses. It provides many element types to the user for implementing. However, using of mixed element type in the analysis is still difficult in linking degree of freedom of different elements. Accordingly, pure 3D multilayered shell element was adopted in all analyses.

*1 Department of Civil Engineering, Nagoya University, Graduate Student, Member of JCI
*2 Department of Civil Engineering, Nagoya University, Professor, Member of JCI
*3 Department of Civil Engineering, Nagoya University, Member of JCI
*4 Department of Civil Engineering, Nagoya University, Graduate Student, Member of JCI

2. PRESTRESSING TENDON FORMULATION

Free body diagram of a segment of prestressing tendon passing an element is shown in **Fig.1**. Cross-sectional area of the tendon is A_p with a tangential Young's modulus of E_{pt}. Both ends crossing the boundary of the element is defined by point P and Q, which are possessing a tangential vector of $\mathbf{t}_P$ and $\mathbf{t}_Q$, respectively. Two internal prestressing forces, namely P_P and P_Q, are acting at these two ends. Component of distributed force along the tangential direction is p_t, normal component heading to the center of curvature is p_n. These two distributed components can be written in vector form as vector $\mathbf{p}$. By using prestressing tendon axial strain-displacement relation, $\varepsilon_p = \mathbf{B}_p\mathbf{a}$, the equilibrium equation based on virtual work concept for prestressing tendon can be written as in eq.(1).

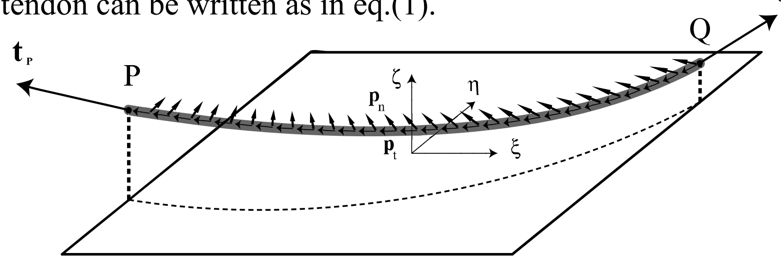

Fig. 1 Free body diagram of tendon segment

$$A_p\left[\int_\Gamma E_{pt}\mathbf{B}_p^T \otimes \mathbf{B}_p ds\right]\mathbf{a} + A_p\int_\Gamma \mathbf{B}_p^T\sigma_{p0}ds = \int_\Gamma \mathbf{N}^T\mathbf{p}dS + P_P\mathbf{N}_P^T\mathbf{t}_P - P_Q\mathbf{N}_Q^T\mathbf{t}_Q \quad (1)$$

where vector **a** denotes a set of nodal displacement of the corresponding element.

Rewriting eq.(1) into more concise form, the equilibrium of prestressing tendon can be expressed in matrix form as in the following equation.

$$\mathbf{K}_p\mathbf{a} + \mathbf{R}_p = \mathbf{P}_p \quad (2)$$

where

$$\mathbf{K}_p = A_p\int_\Gamma E_{pt}\mathbf{B}_p^T \otimes \mathbf{B}_p ds\,,\ \ \mathbf{P}_p = \int_\Gamma \mathbf{N}^T\mathbf{p}dS + P_P\mathbf{N}_P^T\mathbf{t}_P - P_Q\mathbf{N}_Q^T\mathbf{t}_Q\,,\ \ \mathbf{R}_p = A_p\int_\Gamma \mathbf{B}_p^T\sigma_{p0}ds \quad (3)$$

In bonded tendon prestressing system, the axial strain-displacement relation matrix $\mathbf{B}_p$ can be obtained by transforming the parent strain field to the axial tendon strain with respected to the moving trihedral. The parent strain field is defined in $\xi\eta\zeta$ coordinate system, which is equivalent to the strain field calculated from reinforced concrete element. The parent strain field is then transformed to moving trihedral system, $\mathbf{tnb}$ system, by using the transformation matrix, $\mathbf{T}$, as $\boldsymbol{\varepsilon}'_{tnb} = \mathbf{T}^T\boldsymbol{\varepsilon}_{\xi\eta\zeta}\mathbf{T}$.

Strain component that is considered in the tendon is only the axial component, ε'_x, which is corresponding to the tangential component, $\mathbf{t}$, of the moving trihedral. By removing the unwanted strain components, the tendon strain (axial strain) can be expressed as in the following equation.

$$\varepsilon_p = \mathbf{C}\left\{\varepsilon_x \quad \varepsilon_\eta \quad \varepsilon_\zeta \quad \gamma_{\xi\eta} \quad \gamma_{\xi\zeta} \quad \gamma_{\eta\zeta}\right\}^T = \mathbf{C}\ _c = \mathbf{CB}\left[\mathbf{x}_p(t)\right]\mathbf{a} = \mathbf{B}_p(t)\mathbf{a} \quad (4)$$

where

$$\mathbf{B}_p(t) = \mathbf{CB}\left[\mathbf{x}_p(t)\right] \quad (5)$$

By a substitution of eq.(5) into eq.(3), stiffness matrix contributed by prestressing tendon for bonded problem can be obtained.

In the case of unbonded prestressing system, the $\mathbf{B}_p$ matrix is more complicated than that expressed by eq.(5). The total increment of concrete along the tendon length shall be equal to total elongation of the prestressing tendon, which can be mathematically expressed as

$$\int_0^l \varepsilon_c ds = \sum_{i=1}^{n} \left[\int_0^{l_i} \mathbf{C}\mathbf{B}_i \left(\mathbf{x}_p (t) \right) ds \right] \mathbf{a}_i = \Delta u_p \tag{6}$$

where ε_c is concrete strain along tendon length, l is a total length of prestressing tendon, n is a total number of element that the prestressing tendon passing through, $\mathbf{B}_i$ is strain-displacement matrix of parent element, and Δu_p is a total elongation of the prestressing tendon.

In the case of no friction is considered, tendon strain shall be the same through the length of the tendon, that is

$$\varepsilon_p = \frac{\Delta u_p}{l} = \frac{\sum_{i=1}^{n} \left[\int_0^{l_i} \mathbf{C}\mathbf{B}_i \left(\mathbf{x}_p (t) \right) ds \right]}{\sum_{i=1}^{n} \int_{-1}^{1} J_p dt} \mathbf{a} \tag{7}$$

Stiffness matrix for unbonded system can also be calculated by using eq.(7). Nevertheless, unlike the bonded case, integration limit should be done upon a total prestressing tendon length, in which the dimension of stiffness matrix is depending on the number of element that the prestressing tendon passing through. Assembling of the stiffness matrix is performed component by component to the global stiffness matrix according to the corresponding degree of freedom.

3. NUMERICAL EXAMPLES

3.1 CONTINUOUS PRESTRESSED CONCRETE BEAM

First analysis is a continuous prestressed concrete beam, which is tested by T.Y. Lin. [2]. Among the beam specimens of his test series, the designated beam B has been selected to verify the concrete constitutive model and finite element model proposed in this research, which is a symmetric continuous prestressed concrete beam containing two equivalent span-lengths and is simply supported bythree hinge supports, as shown in **Fig. 2 (**the figure is not in proportion**)**. The beam cross-section is rectangular with the size of 203×406 *mm*. One prestressing tendon is placed in the curve line with eccentricity at the plus-moment and minus-moment zone. The beam is subjected to two point-loads at about one-third position in each span.

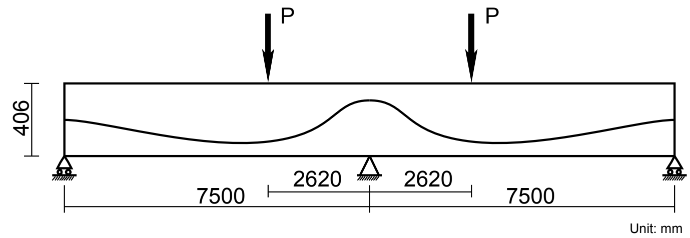

Fig. 2 Continuous prestressed concrete beam geometry

Main reinforcing bar is located at four corners of the beam, having diameter of 14 *mm*. If letting the z-axis heads upward starting from the lower extreme fiber, location of the prestressing tendon will be described as: z = 203 *mm* at both ends, z = 155 *mm* at loading point, z = 300 *mm* at the middle support.

Full structure is modeled into finite element mesh using 240 5-layers shell elements. The curved prestressing tendon is interpolated by B-spline interpolation. The unbonded prestressing formulation is applied to the general finite element formulation. Mechanical properties used in the analysis are shown in **Table 1**.

Vertical load P is monotonically increased. Load and corresponding vertical displacement at the load point relation is shown in **Fig. 3**. In addition, incremental force ΔP caused by prestressing force was deducted from the applied force in order to represent the vertical axis in **Fig. 3** as an additional applied force only. The figure shows comparison between analysis result (solid line), experimental result (dotted line), and analysis result when no prestressing stress is applied (grayed solid line).

Both analysis results possess nearly the same initial slope as of the experiment. In the case of no prestressing stress, the load-displacement curve deviated from the experimental result when the applied load reached around 20 *kN*. When the prestressing stress is applied to the tendon with the value of 1060.1 N/mm^2, the analysis result is almost coincided the experimental result until the applied load has reached around 140 *kN*. Some deviation can be seen when the applied load increased. However, the estimation of maximum strength is satisfactory obtained.

Concrete		
	Young's modulus	37,100 N/mm^2
	Compressive strength	38 N/mm^2
	Tensile strength	4.9 N/mm^2
	Cracking strain	0.002
	Poisson ratio	0.0
Reinforcing steel		
	Young's modulus	198,800 N/mm^2
	Yielding stress	318.5 N/mm^2
Prestressing tendon		
	Cross-sectional area	621.3 mm^2
	Young's modulus	202,222 N/mm^2
	Prestressing stress	1060.1 N/mm^2

Table 1 Mechanical properties of prestressed concrete beam

Fig. 4 shows the deformation of the beam and crack pattern, only half of the beam is shown, at the point when the applied load reached its maximum value. The leftmost end, which the prestressing load directly applied, shows some cracks due to compression failure. Bending cracks occurred at the mid-span lower fiber and horizontal cracks at the mid-span upper fiber caused by confining effect, the force component normal to the tendon course, from prestressing tendon.

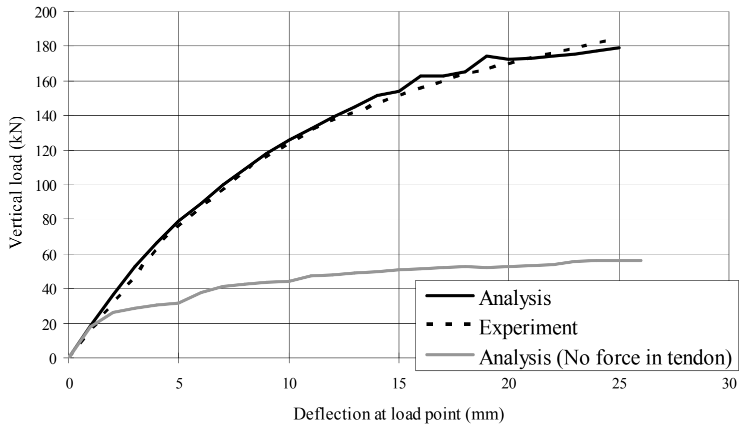

Fig. 3 Load-displacement diagram of PC beam

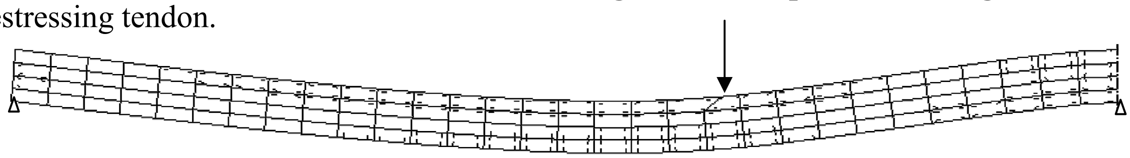

Fig. 4 Deformation and crack pattern of the prestressed beam

3.2 I-SHAPE PRESTRESSED CONCRETE BEAM

Series of prestressed beam that were studied in this subsection were built and tested by cooperating between Civil engineering laboratory, Ministry of Construction and Japan Prestressed Concrete Engineering Association [3].

Four internal-cable prestressed concrete beams with different geometric parameters see **Table 2**, have a common geometry as in the follows. The beam having a total length of 8000 *mm* was simply supported with a span length of 7000 *mm*. Cross-section of the beam is a symmetric I-shape with a full height of 1100 *mm*, flange width of 500 *mm*, flange thickness of 150 *mm*, and web thickness of 150 *mm*. For the longitudinal reinforcement, four D22 bars and six D22 bars were used in upper-flange and lower-flange, respectively. Excluding beam S6 (beam without stirrup), D10 bars with a spacing of 200 *mm* were used as a stirrup. **Fig. 5** shows the geometry and reinforcement detail for common beam (beam in the figure is an externally prestressed beam which is excluded from the analysis).

Four prestressing cables installed in each beam are 1S21.8 (SWPR7AL) type with an initial prestressing stress of 850 N/mm^2 (excluding S7 beam, no prestressing stress is applied).

Specimen	PC cable		Cable angle		Stirrup		Prestressing	
	internal	external	0°	5°	standard	none	PC	RC
S2	X			X	X		X	
S4	X		X		X		X	
S6	X			X		X	X	
S7	X		X		X			X

Table 2 List of prestressed concrete beam specimens

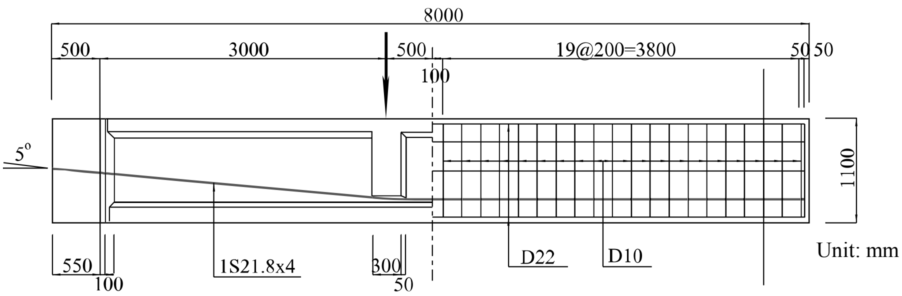

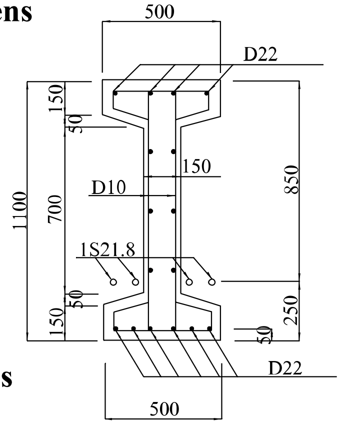

Fig. 5 Geometry and reinforcement detail of beam specimens

Two points monotonic vertical load was equally applied at the 500 *mm* position away from midspan. Concrete and reinforcement properties used in the experiment and analysis are listed in **Table 3**.

Concrete				
	Specimen	Compressive strength (N/mm^2)	Tensile strength (N/mm^2)	Young's modulus (N/mm^2)
	S2	46.7	4.091	31,090
	S4	44.0	3.799	28,650
	S6	57.5	4.186	30,090
	S7	53.4	4.097	28,770
Reinforcement and prestressing tendon (same for all specimens)				
	Reinforcement	Yielding stress (N/mm^2)	Tensile strength (N/mm^2)	Young's modulus (N/mm^2)
	D22	382	542	188,100
	D10	360	560	188,100
	1S21.8	1692	1801	217,000

Table 3 Mechanical properties of prestressed concrete beams

Half model of all beam specimens were analyzed by using the procedures proposed in previous sections. Applied load and vertical deflection at the mid-span relations are shown in **Fig 6** and **Fig 7**. Beam S2 and S4 are different by prestressing cable angle, and it does not affect much to the ultimate strength of the beams. Beam S2 reached the ultimate strength at 1850 *kN* when deflection is 55.4 *mm*, and beam S4 at 1812 *kN* when deflection is 51.6 *mm*. These two beams are failed by shear failure. The analysis results are represented by solid line. Initial stiffness from the analysis of both beams are very close to that of the experiment until applied load reached about 600 *kN*. After the first occurrence of bending cracks (~600 *kN*), longitudinal reinforcement and prestressing tendon stiffness contributed stiffness of the whole structure. In the analysis, the result is a bit stiffer than that of the experiment after the first deviation. The load-deflection curve deviates again when applied load reached about 1350 *kN* (reinforcement in tension zone is about to yield). Beam specimen S2 and S4 are suddenly failed by shear failure when mid-span deflection is 67 *mm* and 51 *mm*, respectively. In the analysis, both beams are also suddenly failed by shear when mid-span deflection is 60.864 *mm* and 53.772 *mm*.

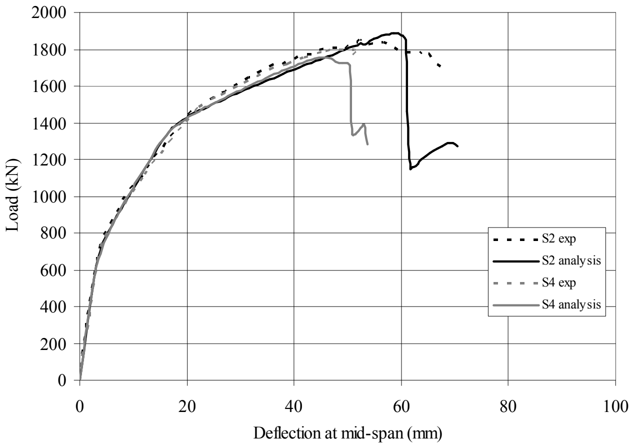

Fig. 6 Load-displacement relations (S2, S4)

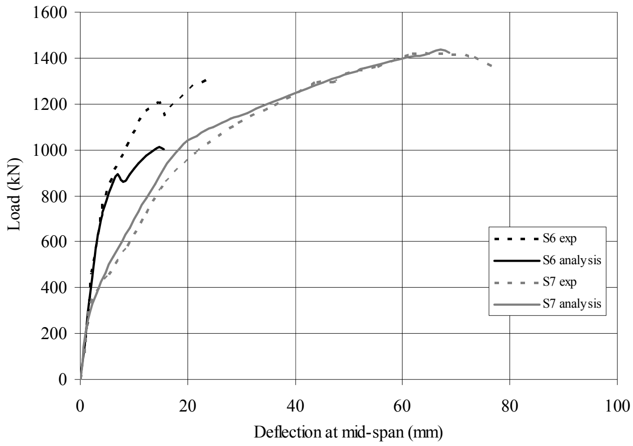

Fig. 7 Load-displacement relations (S6, S7)

Beam S6 (no stirrup) analysis result, as shown in **Fig. 7**, is relatively well predicted until the applied load reaches about 900 *kN*. With addition of the vertical load, beam from the analysis result suddenly failed by shear failure when deflection is 6.9 *mm*, while beam specimen continues to resist the load and failed at about 1200 *kN* when deflection is 14.6 *mm*.

Beam S7 (no prestressing load) has ultimate strength of about 1400 *kN* while it strength can be increased to 1850 *kN* when prestressing load is applied. Stiffness of the beam decreased when first bending crack occurred (225 *kN*) and decrease furthermore when shear cracks appeared (349 *kN*). The analysis result is moderately stiffer after the first deviation. An ultimate strength of the beam specimen is reached when applied load is about 1418 *kN* when deflection is 61 *mm* and failed when deflection is 77.5 *mm*. The ultimate strength can be well predicted by the analysis, 1430 *kN*, with the deflection at failure equal to 68.76 *mm*.

4. CONCLUSIONS

By introducing of the prestressed concrete formulation accompanied with the reinforced concrete formulation (LECM) to the nonlinear FEM, behavior of the prestressed concrete component can be well predicted. However, the correctness of the analysis is also depending on modeling and discretization of the structure. Further development shall be carried out in order to study the more complicated prestressed concrete structural components.

REFERENCES

1. Bongochgetsakul N. and Tanabe T., “Analysis of Box Type Shell Structures under Cyclic Loading by Lattice Equivalent Continuum Model”, Transactions of the JCI, Vol. 24, 2002, No. 2, pp. 949-954.
2. T.Y. Lin, “Strength of Continuous Prestressed Concrete Beams under Static and Repeated loads”, ACI journal, Vol. 26, 1955, No. 10.
3. Nishikawa K., Hiromatsu S., Itou K., ”外ケーブルを適用した PC げたのせん断挙動に関する実験”, Journal of prestressed concrete, Proceedings of the 10th symposium, October 2000, pp. 511-516.